


Article

Spatiotemporal Patterns of Carbon Emissions and Taxi Travel Using GPS Data in Beijing

Jinlei Zhang ¹, Feng Chen ^{1,2}, Zijia Wang ^{1,*} , Rui Wang ¹ and Shunwei Shi ¹

¹ School of Civil and Architectural Engineering, Beijing Jiaotong University, No.3 Shangyuancun, Haidian District, Beijing 100044, China; 17115275@bjtu.edu.cn (J.Z.); fengchen@bjtu.edu.cn (F.C.); 16115261@bjtu.edu.cn (R.W.); 16121207@bjtu.edu.cn (S.S.)

² Beijing Engineering and Technology Research Center of Rail Transit Line Safety and Disaster Prevention, No.3 Shangyuancun, Haidian District, Beijing 100044, China

* Correspondence: zjwang@bjtu.edu.cn; Tel.: +86-010-5168-8070

Received: 21 December 2017; Accepted: 19 February 2018; Published: 27 February 2018

Abstract: Taxis are significant contributors to carbon dioxide emissions due to their frequent usage, yet current research into taxi carbon emissions is insufficient. Emerging data sources and big data-mining techniques enable analysis of carbon emissions, which contributes to their reduction and the promotion of low-carbon societies. This study uses taxi GPS data to reconstruct taxi trajectories in Beijing. We then use the carbon emission calculation model based on a taxi fuel consumption algorithm and the carbon dioxide emission factor to calculate emissions and apply a visualization method called kernel density analysis to obtain the dynamic spatiotemporal distribution of carbon emissions. Total carbon emissions show substantial temporal variations during the day, with maximum values from 10:00–11:00 (57.53 t), which is seven times the minimum value of 7.43 t (from 03:00–04:00). Carbon emissions per kilometer at the network level are steady throughout the day (0.2 kg/km). The Airport Expressway, Ring Roads, and large intersections within the 5th Ring Road maintain higher carbon emissions than other areas. Spatiotemporal carbon emissions and travel patterns differ between weekdays and weekends, especially during morning rush hours. This research provides critical insights for taxi companies, authorities, and future studies.

Keywords: taxi GPS data; carbon emission; dynamic spatiotemporal distribution; kernel density analysis

1. Introduction

With improved information and communication technologies, as well as location-based services (LBS) such as mobile phone communications, social software, vehicle-carried GPS (Global Position System) positioning terminals, etc., large-scale, high-quality, and consecutive spatiotemporal trajectory data on urban mobility has become an increasingly popular dataset and principal resource. Many researchers employ advanced data mining techniques and big geospatial data, among which taxi GPS data is one of the prevailing resources, to analyze individual travel patterns, the organization and planning of urban public spaces, construction of smart cities, and so forth. At present, studies using taxi GPS data include, but are not limited to, the following aspects: route planning and path-finding, traffic operational state identification, identification of origin-destination (OD) and the clustering method, and taxi fuel consumption and emissions estimation. The typical and important current researches are summarized in Table 1.

Previous studies have extracted experiential driving route sets from taxi trajectories, built experiential road hierarchies according to the driving experiences of taxi drivers, such as travel frequency and speed information for different road segments at different times, and proposed

hierarchical path-planning methods to determine the optimal paths to support dynamic route planning or path-finding [1–6].

Furthermore, because of their low cost, wide coverage, easy data access, accurate allocation, high continuity, and, most importantly, their feasibility, big taxi GPS data can also identify the traffic state [7,8]. This includes exhaustive analyses of spatiotemporal congestion patterns on urban roads [9] and measurements of traffic jam indicators [10], allowing for a better understanding of the operational states of road networks. Moreover, by proposing different and effective anomaly detection methods, some studies have used the taxi dataset to detect anomalous traffic events, which occur when the corresponding indicators deviate significantly from the expected values [11], and to detect anomalous routes such as fraudulent taxi travel patterns or traffic accidents, as well as identifying the parts of the trajectories responsible for the anomalies and ranking them with an ongoing anomaly score [12]. Other studies have monitored unexpected behaviors, such as vehicle breakdowns, or one-time events like large sporting events, fairs, and conventions, which exhibit the largest statistically significant departure from expected behavior [13]. Additional research has estimated the average relationship between travel time and driving speed [14–16].

Through identification of origin-destination (OD) and the clustering method, some researchers have attempted to detect urban passenger hotspots, i.e., taxi demand prediction [17,18], and then provide location recommendation services for empty taxis [19,20]. By establishing an OD taxi travel matrix, Xin et al. [21] focused on the recognition of commuter behavior, along with employment and residential areas, based on taxi trajectory data. In addition, using OD data, taxi trip characteristics can be evaluated, including their temporal and spatial distribution [22].

To date, research into fuel consumption and taxi emission calculations using big data-mining techniques and taxi trajectories has been relatively rare. For example, by obtaining the average speed of trajectory segments, Luo et al. [23] computed taxi energy consumption and emissions, and analyzed their spatiotemporal distribution in Shanghai via ArcGIS software. However, the study did not consider variations in carbon emissions per kilometer (CEPK), fuel consumption per 100-km (FCPOK), or the average travel speed over the whole network during the calculation, which are the global, standard, and intuitive indicators, nor did it verify the accuracy of the results. Moreover, their data only covered 20% of all taxis in Shanghai. In this study, we analyze more than 50% of all taxis in Beijing, thereby providing more credible insights for urban planning and traffic management authorities. Du et al. [24] applied floating vehicle data to predict vehicle fuel consumption using a Back Propagation Neural Network. They also compared the difference in fuel consumption distribution within downtown Beijing between weekdays and weekends using a heat map. However, this study only involved the total fuel consumption and did not analyze its variation throughout a day, nor did it include carbon emission patterns. Other researchers conducted a bench test to obtain fuel consumption and emissions from taxi GPS trajectory data [25] but did not fully take advantage of big data-mining techniques and employed only one car model of the current taxi, the Hyundai Elantra taxi, which could not reflect the effects of most car models in Beijing. In this study, we include more than five car models of the current taxi.

With the availability of more detailed data and big data-mining techniques, taxi carbon emissions can be addressed at a much higher resolution, and more factors can be considered, such as the impact of average speed on emissions, in order to overcome the limitations of previous studies. To this end, this study establishes an analytical framework to calculate and present taxi emissions that can be adapted to big data resources and tools. First, we describe the data sources and the reconstruction of taxi trajectories employing taxi GPS data along with Oracle (Oracle 11g, Oracle, Redwood City, CA, USA) and ArcGIS (ArcGIS 10.3, Esri, Redlands, CA, USA) software. Second, this study introduces a carbon emission calculation model based on the fuel consumption calculation algorithm using the Vehicle Specific Power (VSP) of taxis and carbon emission factors to calculate taxi carbon emissions over the whole network [26]. Third, a visualization method called kernel density analysis is formulated in detail to obtain the dynamic spatiotemporal distribution of carbon emissions.

Then, this methodology is applied to Beijing. We calculate taxi fuel consumption over the whole network in Beijing, compute carbon emissions via the carbon emission factor, and then present the dynamic spatiotemporal distribution as maps. To verify the accuracy of the results, we creatively convert carbon emissions and fuel consumption into CEPK and FCPOK, respectively, which are more global, standard, and intuitive factors. The dynamic spatiotemporal distribution of carbon emissions and taxi travel patterns on weekdays and weekends are then highlighted. Finally, the limitations of this research and potential future research areas are proposed.

2. Methodology

In this section, we formulate the methodological framework used in this study. First, we process the taxi GPS data to enable its direct use in the next step. Second, using the carbon emission calculation model based on a taxi fuel consumption algorithm and emission factors, we calculate the carbon emissions over the whole network. Finally, a visualization method called kernel density analysis is applied to obtain the spatiotemporal dynamic distribution of carbon emissions.

2.1. Description and Data Cleaning of Taxi GPS Data

Currently, taxis in many cities are equipped with vehicle information collection devices such as GPS systems. There were approximately 65,000 taxis in Beijing in 2014, and the proportions of different car models of the current taxi are shown in Figure 1 [27]. The data used in this study come from GPS devices installed in taxis, which send information such as taxi identification, coordinates, time, driving speed, and passenger state to the taxi control center every 30 to 60 s. It covers approximately 30,000 to 40,000 vehicles, including more than 30,000 taxis, 5000 to 8000 sightseeing vehicles, and all car models of the current taxi in Beijing. These taxis account for approximately 50% of all taxis in Beijing and produce approximately 40 million records every day. We choose a typical workday and the weekend to comprehensively analyze temporal variations. An example of the dataset is shown in Table 2.

The data are stored in Oracle and, thus, are easily dealt with using the connection between Oracle (Oracle 11g, Oracle, Redwood City, CA, USA) and ArcGIS (ArcGIS 10.3, Esri, Redlands, CA, USA) software. For example, we clean records with invalid locations, those whose coordinates deviate significantly within a few seconds, and those whose speed is always at zero. We delete repetitive records and convert some fields to enable its direct use in the next step, thus reducing the data scale, as well as improving result accuracy and computing efficiency. We then match data points to spatial coordinates using the geographic map in ArcGIS, after which the “Track intervals to line” tool is applied to obtain taxi trajectories with an average speed, which are used later to obtain the fuel consumption, the distance, and driving duration between two adjacent points of the same taxi. Through the reconstructed taxi trajectories shown in Figure 2, we obtain the structure of the road network in Beijing (Figure 3), which corresponds closely to the actual road network.

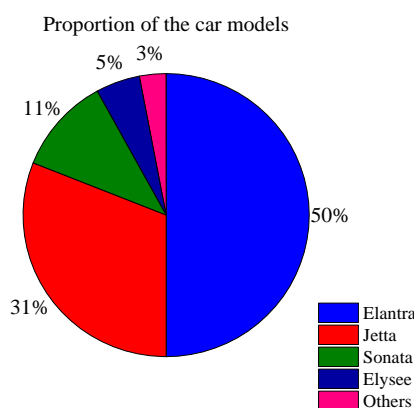


Figure 1. Proportion of different car models of the current taxi in Beijing.

Table 1. Summary of current typical research.

Aspects	Authors	Data Source	Methodology and Contents	Findings and Applications
Route planning and path-finding	Yang et al. (2016) [1]	Shenzhen, China; 12,448 taxis; 75.94 million trajectory points.	Build space-time trajectory cube; Origin-destination constrained experience extraction methods; Generate space-time constrained graph;	Effectively extract the driving experience to support path-finding and dynamic path planning; Road segment global frequency is not appropriate for representing driving experience in route planning models.
	Zhang et al. (2016) [2]	Nanjing, China; 5 million records.	Path selection algorithm based on probability; Improved Prim path selection algorithm; Improved Prim path selection algorithm based on probability; Shortest Path Faster Algorithm.	Improved Prim path selection algorithm based on probability is more optimal in producing an efficient driving route.
	Lin et al. (2015) [3]	Beijing, China; more than 3000 taxis.	Build a hierarchical road network; Path planning method based on experience.	Experienced routes are selected with considering all factors especially with saving more travel time.
Traffic operational state identification	Zhang et al. (2017) [9]	Shanghai, China; 58,000 taxis; 114 million records.	Identify traffic congestion; Investigate the relationship between traffic congestion and built environment; Fuzzy C-means clustering and spatial autoregressive moving average model.	Find that continuous congestion often happens in city centre and factors such as road type, bus station, ramp nearby and commercial land use have large impacts on congestion formation.
	Kong et al. (2015) [10]	Shenzhen, China; 13,798 taxies; 20 million records.	Introduce a travel time index (TTI) to measure the level of congestion; Compute TTI in different time intervals and roads;	TTI is a traffic congestion indicator with fine-grained spatial and temporal accuracy and can be used in many other cities to evaluate traffic conditions.
	Kuang et al. (2015) [11]	Harbin, China; 15,000 taxies;	Using taxi GPS data to build traffic flow matrix; Anomaly detection method was proposed based on wavelet transform and principal component analysis;	Anomalous traffic events can be detected when corresponding indicators deviate significantly from the expected values.
	LI et al. (2014) [14]	Nanjing, China;	Proposing a link travel time estimation method without signal timing data.	The average absolute error and relative error of this method is 12 s and 8.67% respectively.
	Pang et al. (2013) [13]	Beijing, China;	statistic detection models based on likelihood ratio test statistic	Monitoring unexpected behaviors such as vehicle breakdowns, or one-time events like large sporting events, fairs, and conventions.
	Chen et al. (2012) [12]	Hangzhou, China; 7600 taxis;	Isolation Based Online Anomaly Trajectory Detection; A real-time method that identifies which parts of a trajectory are anomalous; Introducing an ongoing anomaly score which can be used to rank the different trajectories.	Detection of fraudulent taxi drivers.

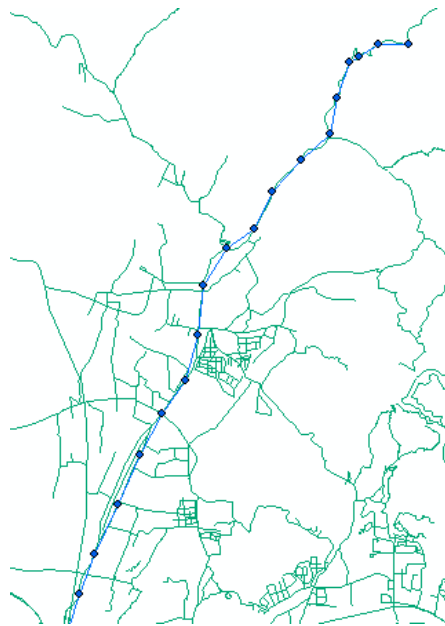
Table 1. Cont.

Aspects	Authors	Data Source	Methodology and Contents	Findings and Applications
Identification of OD and the clustering method	Zhao et al. (2015) [17]	Wuhan, China; 3000 taxis.	Proposing a method of trajectory clustering based on decision graph and data field.	The hotspots in different time in holiday, weekday, and weekend are discovered and visualized in heat maps; Taxi demand prediction.
	Shen et al. (2015) [20]	Nanjing, China; 7600 taxis.	Using an improved DBSCAN algorithm in hot spot extraction; Defining weighted tree including factors of distance, driving time, velocity and end point attractiveness in route evaluation.	Providing recommendation to help cruising taxi drivers to find potential passengers with optimal routes.
	Xin et al. (2017) [21]	Xi'an, China;	Establishing a travel OD matrix based on traffic analysis zone; Proposing a commute identification model based on trajectory data; Establishing a commute time and distance computing model; Analysis of spatiotemporal characteristics of commute behavior.	Identification of commute behavior using taxis, workplace and residence. Optimization of traffic system for commuter services.
Taxi fuel consumption and emissions estimation	Luo et al. (2016) [23]	Shanghai, China; 13,675 taxis; 140 million records.	Fuel consumption and emissions calculation model; Mapping technique for spatial distribution of emissions.	The distribution characteristics of emissions including CO, HC, NOx, and fuel consumption in Shanghai.
	Du et al. (2017) [24]	Beijing, China; 13,000 floating vehicles.	Using a Back Propagation Neural Network to establish a fuel consumption forecasting model.	Exploring the fuel consumption pattern and congestion pattern; Probing drivers' information and vehicles' parameters; The spatiotemporal characteristics of average speed and average fuel consumption; The difference in fuel consumption distribution within downtown Beijing between weekdays and weekends.
	Weng et al. (2017) [25]	Energy Testing Center of Motor Transport Industry of Ministry of Transportation, China.	A bench test involving three driving cycles: cruising, acceleration and deceleration, and the composite driving cycle including these two; Proposing a model to calculate fuel consumption and emissions based on the driving trajectory reconstruction.	The fuel consumption and emissions can be gotten from second-by-second GPS data.

Table 2. Example of taxi GPS data.

Taxi ID	Positioning Time	Latitude	Longitude	Speed (m/s)	Passenger State	Description
1379	2014/6/18 11:50:00	39.91004	116.30812	11.83	268435456	closed door, effective location, occupied.
1379	2014/6/18 11:51:01	39.9099	116.31544	9.26	268435456	closed door, effective location, occupied.
1379	2014/6/18 11:52:00	39.9097	116.32033	0	268435456	closed door, effective location, occupied.
1379	2014/6/18 11:53:00	39.90942	116.32373	9.77	268435456	closed door, effective location, occupied.
1379	2014/6/18 11:54:00	39.9098	116.3285	3.08	268435456	closed door, effective location, occupied.
1380	2014/6/18 5:38:20	39.91548	116.18801	4.11	0	closed door, effective location, vacant.
1380	2014/6/18 5:39:21	39.91453	116.18817	2.05	0	closed door, effective location, vacant.
1380	2014/6/18 5:40:20	39.9143	116.19248	4.63	0	closed door, effective location, vacant.
1380	2014/6/18 5:41:19	39.91246	116.19693	8.74	0	closed door, effective location, vacant.

In the passenger state column, “268435456” means there is at least one passenger in the taxi and “0” means the taxi is vacant.

**Figure 2.** An example of taxi trajectories in Beijing.

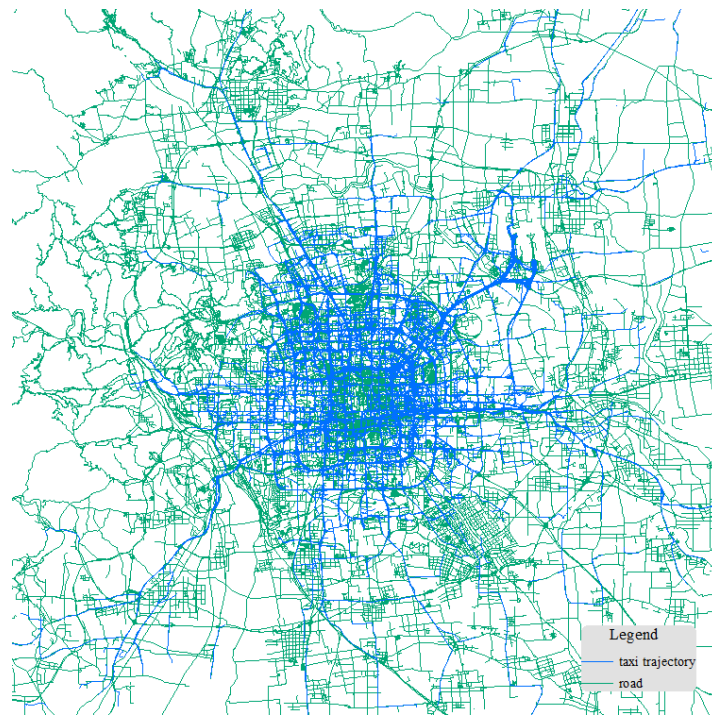


Figure 3. Reconstructed structure of the road network in Beijing from taxi trajectories.

2.2. Carbon Emission Calculation Model

Vehicle Specific Power (VSP), which indicates the output power of the engine when it moves a ton of weight, including its own, was first proposed by Jiménez-Palacios in his doctoral dissertation in 1999 [28]. We obtain the VSP from vehicle speed and acceleration.

$$\text{VSP} = v \cdot (1.1 \cdot a + 9.81 \cdot \text{grade}(\%) + 0.132) + 0.000302 \cdot v^3 \quad (1)$$

where v and a are the speed (m/s) and acceleration (m/s²), respectively, and grade represents the road grade, which is assumed to be zero in urban road networks.

Compared with speed and acceleration, fuel consumption has a stronger correlation with VSP [29–31]. In practice, however, we cannot easily obtain the exact running state of a vehicle, especially the speed per second, required to compute the VSP, because it will cause high costs for the taxi operational company if it tries to obtain the exact running state of a vehicle. Therefore, a more accurate fuel consumption estimation is less likely. To overcome this shortcoming, Song and Tu [26,32] performed experiments to explore the relationship between VSP and fuel consumption and how to more meaningfully obtain the VSP and fuel consumption from the average speed, which is easier to acquire. The relationship between the average speed and the normalized fuel consumption rate (NFCR) [26] is shown in Table 3.

Table 3. Normalized fuel consumption rate (NFCR) according to average speed interval.

Index	Average Speed Interval (km/h)	NFCR	Index	Average Speed Interval (km/h)	NFCR
1	0–2	1.085137	18	34–36	2.338148
2	2–4	1.258708	19	36–38	2.361389
3	4–6	1.311138	20	38–40	2.395369
4	6–8	1.477515	21	40–42	2.441831
5	8–10	1.573123	22	42–44	2.470396
6	10–12	1.64575	23	44–46	2.538255
7	12–14	1.729985	24	46–48	2.566097
8	14–16	1.807417	25	48–50	2.581801

Table 3. Cont.

Index	Average Speed Interval (km/h)	NFCR	Index	Average Speed Interval (km/h)	NFCR
9	16–18	1.841056	26	50–52	2.595985
10	18–20	1.922954	27	52–54	2.6796
11	20–22	1.996735	28	54–56	2.715854
12	22–24	2.045498	29	56–58	2.755036
13	24–26	2.092286	30	58–60	2.809524
14	26–28	2.163184	31	60–62	2.864735
15	28–30	2.186922	32	62–66	2.956168
16	30–32	2.25144	33	66–70	3.049095
17	32–34	2.328849	34	70–80	3.289347
			35	Above 80	3.550955

Based on Table 3 and the average speed and driving duration obtained from taxi trajectories in ArcGIS, the carbon emissions can be calculated through Equation (2).

$$E_{k,j} = EF_k \cdot \sum_s (ER_0 \cdot \sum_{i=1}^{35} NFCR_i \cdot T_{i,j}) \quad (2)$$

From Equation (2), the fuel consumption can be computed through Equation (3).

$$Q_{s,j} = ER_0 \cdot \sum_{i=1}^{35} NFCR_i \cdot T_{i,j} \quad (3)$$

where $Q_{i,j}$ (g) is the actual fuel consumption in each road segment s of taxi j . ER_0 (g/s), which is calculated as 0.274 g/s using the average value of three car models of the current taxi in [26], is the average fuel consumption rate when VSP is equal to 0. $NFCR_i$ is the non-dimensional normalized fuel consumption rate in the average speed interval i . $T_{i,j}$ is the driving duration in the average speed interval i of taxi j . After obtaining the fuel consumption of each segment s , the total fuel consumption and the corresponding carbon emissions are obtained according to Equation (2).

$$Q_j = \sum_s Q_{s,j} \quad (4)$$

$$E_{k,j} = Q_j \cdot EF_k \quad (5)$$

where Q_j is the total fuel consumption of taxi j , $E_{k,j}$ is the emissions of exhaust k , and EF_k is the emission factor of exhaust k . The IPCC provides the emission factors (693,000 kg/TJ) of carbon dioxide for motor gasoline [33]. According to the calorific value (43,040 KJ/kg) and density (0.73 kg/L) of gasoline, which is the 93# gasoline at 20 °C, obtained from the China Statistical Yearbook [34], the carbon dioxide emission factors (693,000 kg/TJ) are transformed into 2.18 kg/L. This value is used in this study.

2.3. Taxi Carbon Emission Visualization Method

To clearly present the distribution of carbon emissions, set as an attribute of the reconstructed taxi trajectory segments in ArcGIS, we calculate the density of trajectory segments weighted by their carbon emission attribute, applying the kernel density tool. Kernel density can create a smooth curved surface over each line, whose value is greatest exactly on the line, and which decreases to zero as the distance increases to the search radius. The search radius is set as 400 m in this study to derive the standard density available for comparison between different results at different times. The volume under the surface is equal to the product of the line length and the weighted field, namely carbon emissions. Globally, each output raster cell is set as 100×100 , and its density is the sum of all kernel surface values above it. Additionally, the length unit is meters, so the default area unit of the density is km/km^2 , which contains the impact of the carbon emission attribute. Finally, different density intervals are represented with specific colors to demonstrate the emission intensity. An illustration of

the kernel surface over a line segment is shown in Figure 4, and a diagram of the kernel analysis result is displayed in Figure 5, in which the darker colors represent greater emissions.

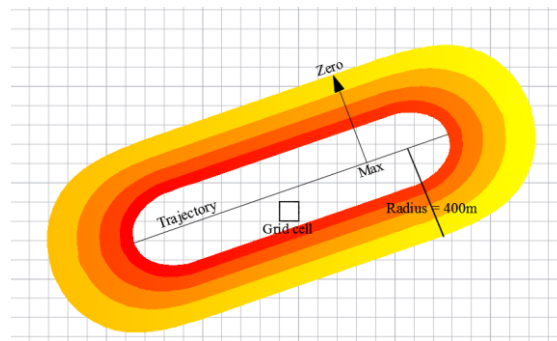


Figure 4. Illustration of the kernel surface over a line segment.



Figure 5. Diagram of the kernel analysis result.

3. Case Study

Beijing is a developed and vibrant mega city with a total city area and central city area in 2014 of 2831 and 939 km², respectively. There are more than 23 million citizens living in Beijing, leading to substantial congestion, especially within the third ring road, where the population density reached 27,000 people per km² in 2014 [35]. As the capital of China, Beijing is the political, economic, cultural, diplomatic, and high-tech innovation center, and residents have easy access to better infrastructure, health care, education, and more working opportunities. Beijing has a hollow, ring-shaped multi center structure, known as a “two-axis, two-belt, and multiple centers” structure; the research area of this study lies mainly within the sixth ring road (Figure 6). The multiple centers refer to the core function regions of the city, including the Zhongguancun High-tech Park (ZHP), Olympic Center District (OCD), Central Business District (CBD), Haidian Science and Technology Innovation Center (HSTIC), Shunyi Modern Manufacturing Base (SMMB), Tongzhou Comprehensive Service Center (TCSC), Yizhuang High-tech Industry Center (YHIC), Shijingshan Comprehensive Service Center (SCSC), and Wang Jing (WJ), called “the first community of the capital” (Figure 6).

Due to increasingly rapid economic and technological development in China, traffic demands have surged rapidly. For example, the motor vehicle and private car population had approached 5.6 and 4.2 million, respectively, by 2014 in Beijing (Figure 7a), and the number of cars per household and per square kilometer are illustrated in [35]. The number of cars has continued to grow, and car density decreases with distance from the center of Beijing (Figure 7b) except for the area in 2nd to 3rd Ring Roads, where car density increases to 55,000/km² [35]. As a consequence, traffic congestion and air pollution become increasingly severe, and the number of motor vehicles and amount of exhaust

emissions must be regulated to relieve traffic jams and improve air quality in Beijing. Therefore, determining the carbon emission patterns of taxis is critical for authorities to make more reasonable management policies, and for taxi companies to promote their operation and management, save operating costs, and most importantly, provide more favorable services for passengers.

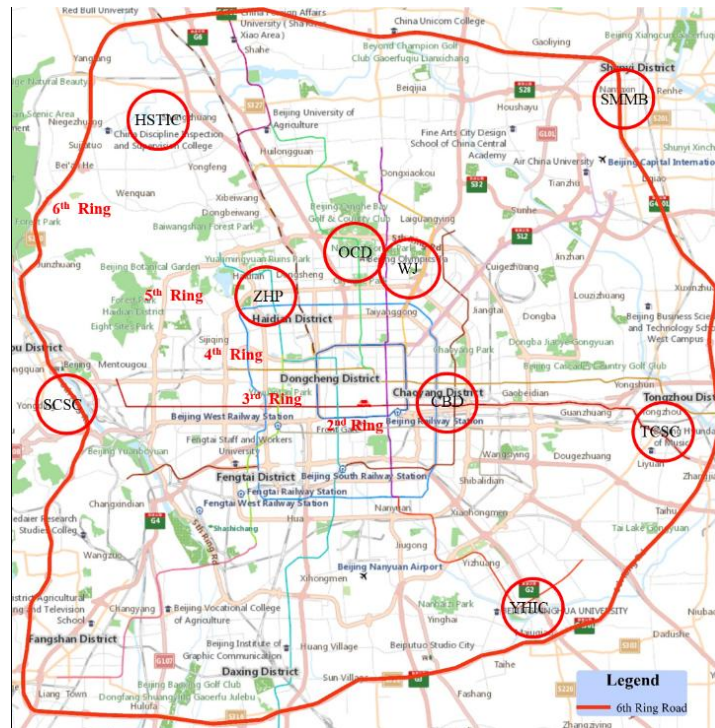


Figure 6. Research area and core function regions of Beijing.

Thus, we analyze the spatiotemporal carbon emissions and taxi travel patterns in Beijing and compare their differences between weekdays and weekends. At a temporal level, we analyze the laws of carbon emissions, fuel consumption, average travel speed, and total travel distance at different time intervals. From the spatial perspective, we analyze the dynamic distribution of carbon emissions at different time intervals. All the differences in these indicators are compared between weekdays and weekends, in the morning and evening rush hour periods.

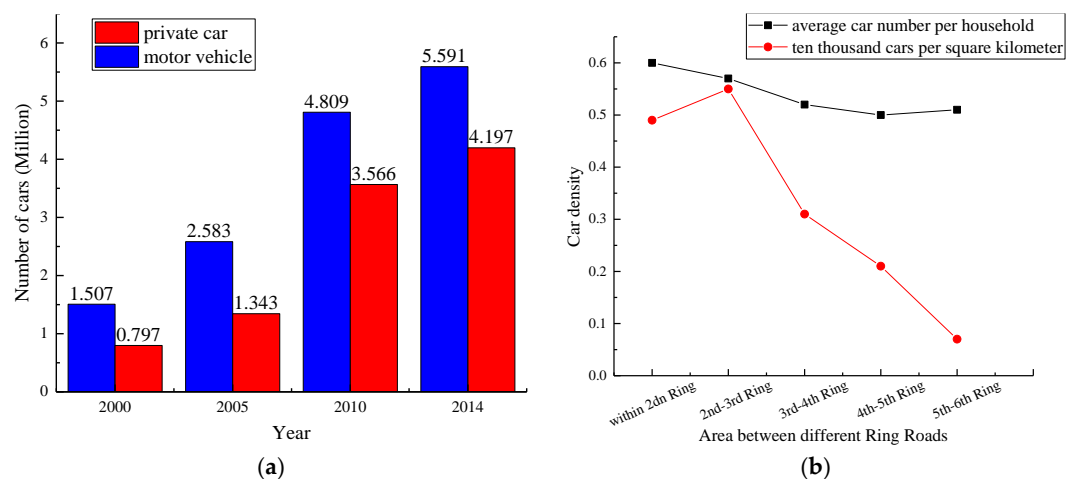


Figure 7. (a) Annual variation of cars and (b) spatial variation of cars with distance from ring roads in 2014.

4. Discussion

4.1. Temporal Carbon Emissions and Taxi Travel Patterns

The number of taxis and records, as summarized in Figure 8, are the most straightforward indicators for representing the global travel patterns of taxis. We can clearly see the travel regularity of taxi drivers in Figure 8, which aligns well with people's expected daily activities.

The number of taxis and records are related throughout the day, with a minimum at 03:00–04:00 when most people are sleeping. The gap between car number and car usage is greatest from 04:00–06:00. Interviews with taxi drivers reveal that most taxi drivers take a shift in this time interval; therefore, not all of them are on full duty. After 06:00, the number of cars on duty climbs to 25,000 cars at 10:00, signifying that many drivers start work during this time interval. Numbers remain stable until 18:00 and then decrease steadily to the minimum. Several specific and typical time intervals are chosen to analyze the spatiotemporal carbon emission patterns in Section 4.3.

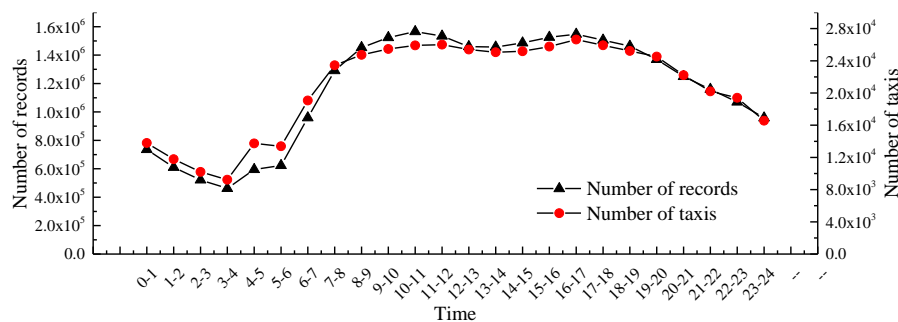


Figure 8. Variation of taxi and record numbers during one day.

To describe carbon emissions in a more standard way, we introduce an indicator named carbon emissions per kilometer (CEPK, kg), calculated according to Equation (6).

$$\text{CEPK} = \frac{\text{Total Carbon Emissions}}{\text{Total travel distance}} \quad (6)$$

The CEPK, which is a global and standard indicator, can evaluate carbon emission levels more objectively, without considering the influence of the individual characteristics and driving conditions of taxis. The total carbon emissions per hour varies substantially during the day (Figure 9), while the CEPK exhibits a slight fluctuation.

Total carbon emissions, in line with the number of taxis, reaches a minimum of 7.43 t from 03:00–04:00. However, they increase by more than seven times during the morning and evening rush hour periods, to 57.53 t and 55.15 t, respectively. CEPK remains relatively stable at approximately 0.20 kg/km throughout the day, yet still increases during rush hour, peaking at 0.26 kg/km from 17:00–18:00. Both total carbon emissions and CEPK then begin to gradually decline. Moreover, both values decrease slightly at 12:00–13:00, when most drivers are on their lunch break. Generally, total carbon emissions in a day reach 965 t, which is a substantial figure.

From this analytical result, it is obvious that the carbon emissions from taxis are huge. Policy makers must issue corresponding regulations to reduce carbon emissions. For example, taxi restrictions in the morning and evening rush hour periods could reduce carbon emissions, ease traffic jam, and encourage people to use public transits. What is more, increasing taxi rental charges during the morning and evening rush hour periods may also be a good policy to ease traffic jams and reduce carbon emissions.

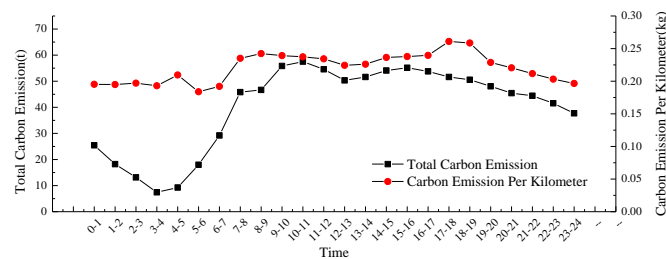


Figure 9. Carbon emissions throughout one day.

The average fuel consumption per 100 km (FCPOK), also a global and well-known indicator, can be calculated according to Equation (7).

$$\text{FCPOK} = \frac{\text{FC} \cdot 100}{L} \quad (7)$$

where FC is taxi's actual fuel consumption (L) and L is taxi's actual driving distance (km) and can be obtained by $v \cdot t$. Therefore, the FCPOK can be obtained according to Equation (8).

$$\text{FCPOK} = \frac{\text{FC} \cdot 100}{v \cdot t} \quad (8)$$

where v is travel speed (km/h) and t is travel time (h).

FCPOK varies substantially from 8.43 L from 05:00–06:00 to 11.97 L from 17:00–18:00 (Figure 10). After 18:00, the average FCPOK slowly decreases with the gradual increase of average travel speed, as shown in Figure 11, which denotes that the travel speed and FCPOK are negatively correlated in a certain range of speed. The average fuel consumption for the entire day is 10.02 L. To verify the analytical result of FCPOK, we sampled 120 taxi drivers randomly, considering the different car models proportions shown in Table 4. Each vehicle corresponds to an FCPOK. The weighted average FCPOK derived from all questionnaires is 8.23 L. The analytical result (10.02 L) is 21.7% more than the figure we investigated (8.23 L).

These results could help policy makers issue stricter regulations related to carbon emission reductions. For example, increasing oil prices may force people to drive less and encourage people to use public transportation or new energy automobiles such as electrical vehicles. To achieve sustainable development, the governments could also command taxi companies to transform the traffic mode of fuel taxis to electrical vehicles or natural gas vehicles so that the carbon emissions can be reduced and living conditions, especially air quality, can be improved. Besides, a restriction policy on private car consumption can reduce fuel consumption and carbon emissions.

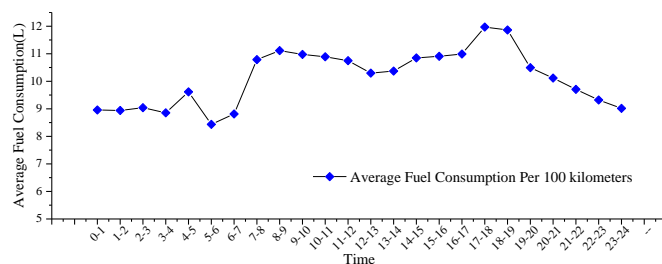


Figure 10. Average fuel consumption throughout one day.

Table 4. Investigated fuel consumption per 100-km (FCPOK) results (L/100 km).

Car Type	Elantra	Zastava	Santana	Sonata	Citroen	Jetta	Weighted Average
number of investigated cars	40	10	10	10	20	30	120
average FCPOK	7.8	9.2	8.5	8.7	8.4	8.1	8.23

The average travel speed and total travel distance are highlighted in Figure 11, which exhibit a roughly negative correlation and considerable fluctuations.

The maximum and minimum average speed is reached from 05:00–06:00 (36.21 km/h) and 17:00–19:00 (21 km/h), respectively. In addition, the travel speed during the morning peak hour period is approximately 25 km/h, slightly higher than during evening peak hours. The average travel speed of the entire day over the whole network is 28.54 km/h. The figure from the Beijing Transportation Development Annual Report is 24.60 km/h, which means that the traffic situation is more serious than previously thought. In contrast, the total travel distance maintains a moderate level during rush hour periods. The maximum travel distance is 67,800 km from 16:00–17:00, which is nearly ten times the minimum of 7400 km from 03:00–04:00. In general, the travel distance in a day reaches up to 4.27 million km.

The average travel speed by hour can be used to monitor traffic conditions throughout an entire urban network. The results indicate that higher resolution travel speed data, such as the average travel speed in one minute, can be obtained to instantly monitor traffic conditions, as long as such a task is feasible for the hardware.

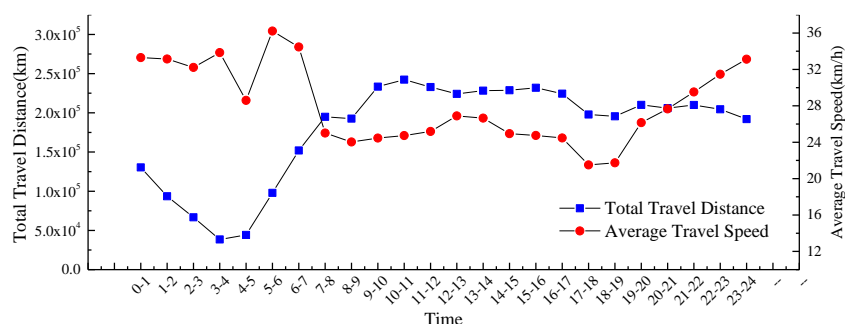


Figure 11. Average travel speed and total travel distance during one day.

4.2. Temporal Comparison of Carbon Emissions and Travel Patterns between Weekdays and Weekends

In terms of CEPK, average travel speed, average FCPOK, and total carbon emissions, we compare the difference between weekdays and weekends in morning and evening rush hour periods as shown in Figure 12. Overall, carbon emissions and travel patterns on the weekend are improved compared to weekdays, regardless of morning or evening rush hour periods.

The average CEPK decrease over all time intervals is approximately 0.03 kg/km, a substantial improvement because it is a relatively microscopic indicator. The average travel speed increases the most on weekend mornings, by 6.3 km/h, and the average FCPOK and total carbon emissions also show the greatest decrease at this time of the weekends, of 1.47 L and 14.5 t, respectively. Values of the average travel speed, average FCPOK, and total carbon emissions at 08:00–09:00 and 17:00–19:00 show relatively fewer variations compared to 07:00–08:00 but also have great improvements between weekdays and weekends. The average improvement across all time intervals is 4.2 km/h, 1.18 L/100 km, and 9.4 t, respectively.

The primary reason for the difference between weekdays and weekends in the morning and evening rush hour periods is that taxi numbers decrease a lot in every time interval—from 24,830 to 21,007, an average decrease of 3823 taxis. Beijing is a megacity, and many people live in the city suburbs. Thus, on the weekdays, most people need to commute between the suburbs and downtown by taxi, which may save more time on the road. On the weekend, however, most people do not need to commute. If they take a taxi on the weekend for a short trip, rather than for their commute into work, they do not necessarily need to get up early, and they can go home at any time.

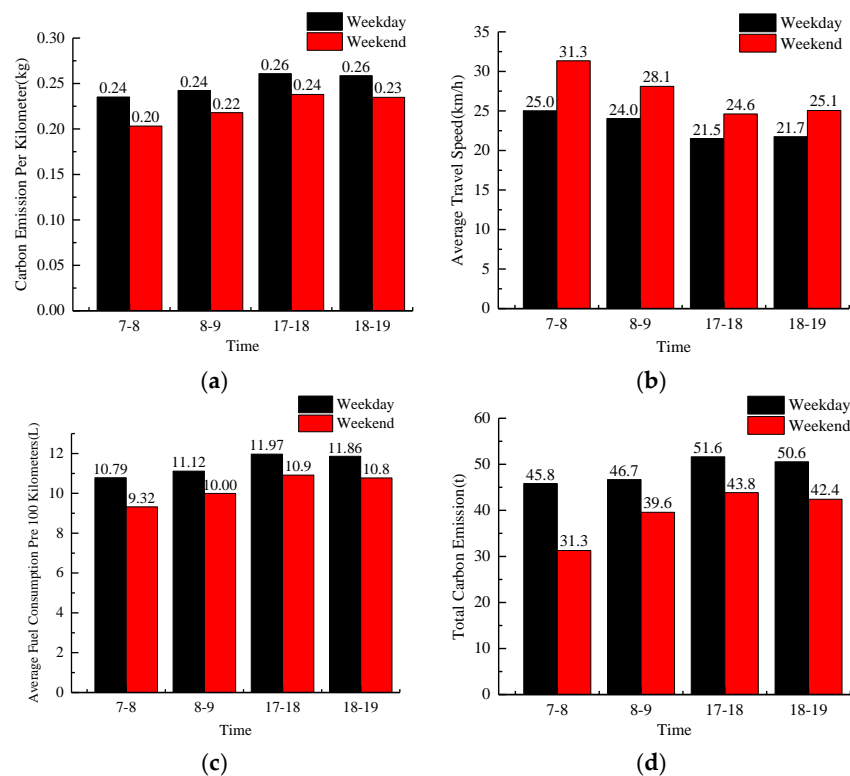


Figure 12. Temporal comparison of carbon emissions and travel patterns between weekdays and weekends. (a) difference in CEPK; (b) difference in average travel speed; (c) difference in average FCPOK and (d) difference in total carbon emissions.

4.3. Spatial Carbon Emission Patterns

After analyzing the temporal carbon emission patterns, we focus on spatial emission distribution characteristics and their dynamic variations with time. Travel activities are mainly distributed within the 6th Ring Road, namely the city center (Figure 13). In fact, carbon emission patterns are highly consistent with the city structure. Therefore, we mainly focus on the area within the 6th Ring Road.

Globally, regardless of the time interval, carbon emissions are highest near the Airport Expressway (S12 in Figure 6) because the Beijing Capital International Airport lies at the northeast end of the Airport Expressway. Therefore, there is a heavy traffic load throughout the day. Carbon emissions are also high on the 2nd, 3rd, and 4th Ring Roads because taxi fleets are common, and drive at higher speeds. Hot spots also appear at intersections of the Ring Road in specific time intervals resulting from large overpasses or interchanges at these locations. Relatively lower carbon emissions happen outside the 5th Ring Road. Most areas bear the effect of many office buildings and high traffic congestion within the 5th Ring Road, which contribute to greater carbon emissions. Moreover, the CBD, TCSC, ZHP, and WJ (Figure 6) are relatively high carbon emission areas due to frequent travel activities. Carbon emissions in the world-famous Palace Museum, situated right in the city center, are quite low, as expected.

From the perspective of time, although the global distribution patterns of carbon emissions do not change substantially, detailed local distributions show distinct variations with time. At the beginning of the day, there is a relatively wide distribution of carbon emissions related to the vibrant night life of a capital city. Then, carbon emissions gradually decrease (indicated by a lighter color in Figure 14) in all regions from 03:00–04:00. From 06:00, they increase at the Airport Expressway and gradually extend to the Ring Roads and particularly to intersections. Notably, carbon emissions increase from the northeast to the southwest with time in the day and decrease in the opposite direction, which

confirms that economic development is higher in the northeast than southwest. From approximately 08:00–09:00, high carbon emissions spread to the expressway, the arterial road, the second trunk road, and even the city streets, until they eventually covering the entire city area, indicating increasingly serious traffic jams during the morning rush hour period. The hot spots at 12:00–13:00, coinciding with relatively low travel distances shown in Figure 11, show lower emissions. Then, the distribution decreases until the evening rush hour period at approximately 19:00, when the color becomes darker than before because people return from work. Following the evening rush hour period, there are no significant changes until midnight, when the cycle starts again. The detailed changes throughout one day can be clearly seen in the supplementary video.

By presenting the spatial dynamic distribution of carbon emissions with time, authorities can instantaneously monitor the distribution of carbon emissions. According to the carbon emissions volume in different regions, authorities can also classify the regional emission grade. Therefore, corresponding carbon emissions reduction measures can be taken in different regions. What's more, the traffic jam spots can be identified so that traffic departments can take related evacuation measures.

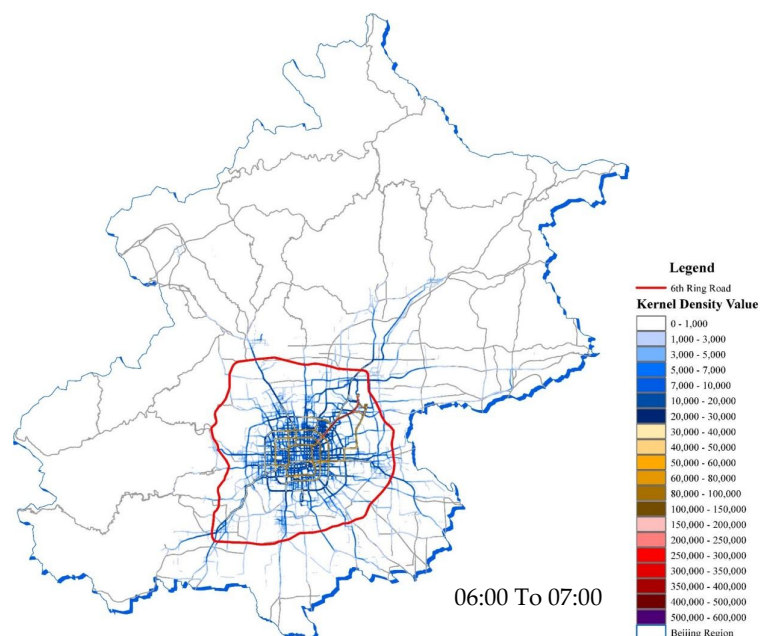


Figure 13. Kernel density analysis results.

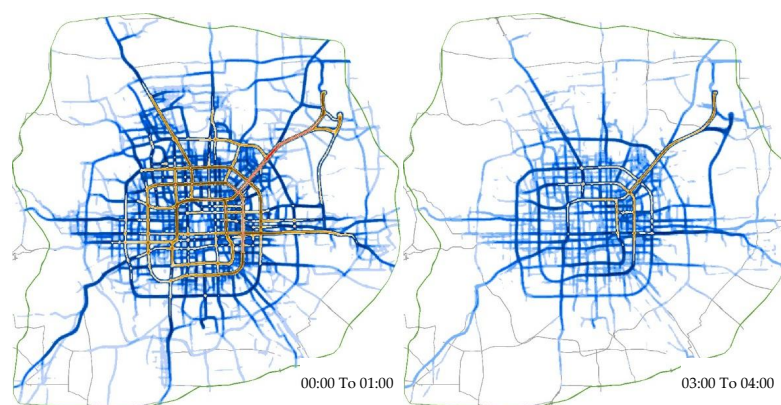


Figure 14. Cont.

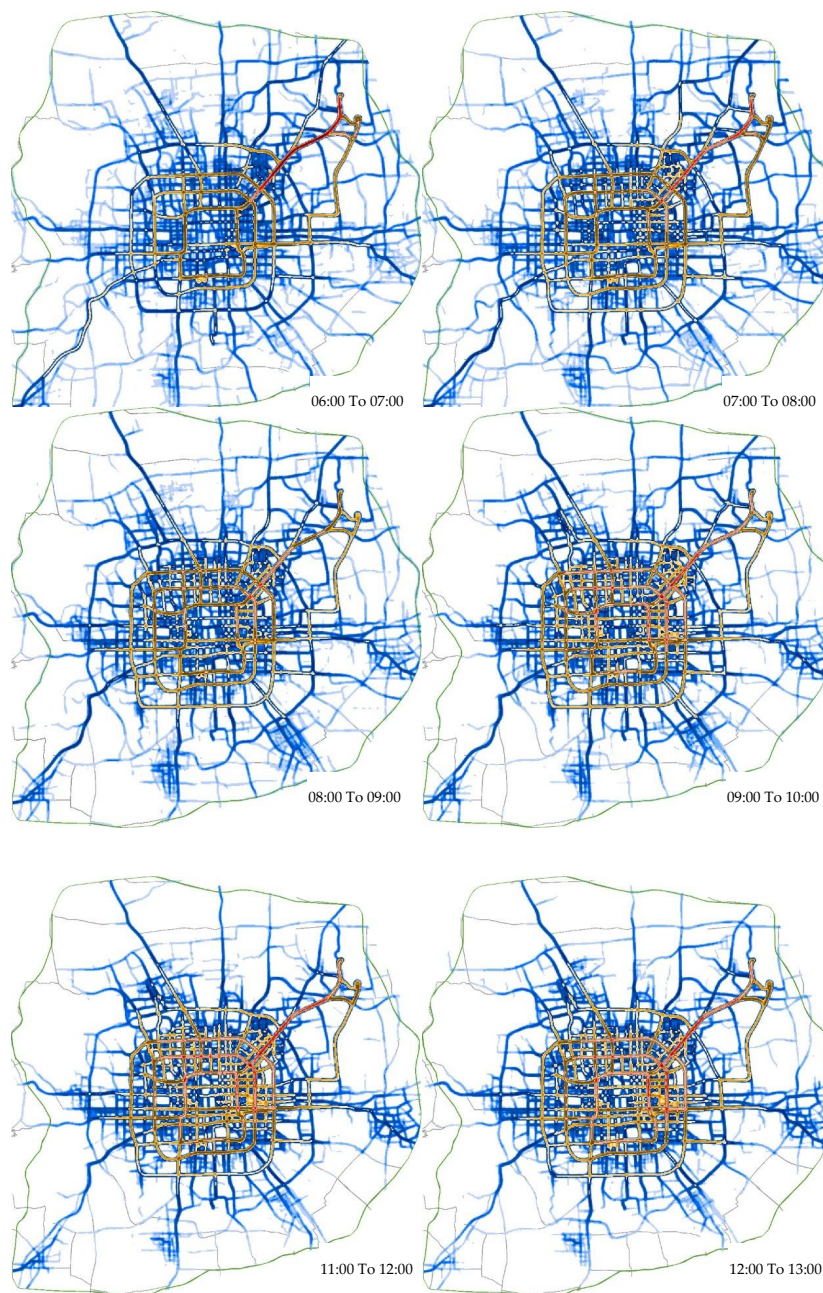


Figure 14. Cont.

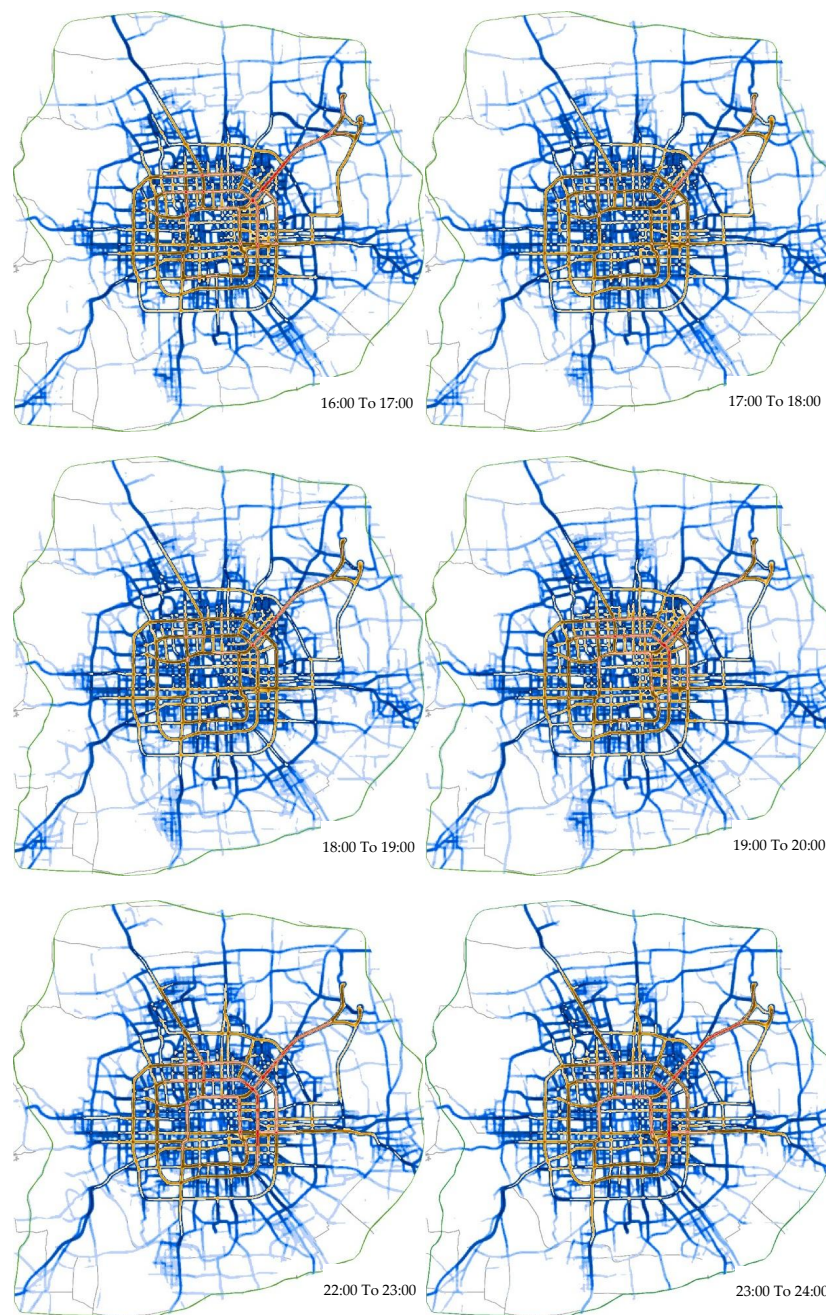


Figure 14. Dynamic distribution of carbon emissions at different time intervals.

4.4. Spatial Comparison of Carbon Emissions between Weekdays and Weekends

Weekday and weekend rush hour periods also exhibit differences in the spatial distribution of carbon emissions, especially in the morning peak hour period, that are similar to the temporal variations (Figure 15).

In general, the weekend exhibits improved carbon emission levels. Emissions in the southwest during the weekend morning peak hour period are substantially lower than on weekdays, especially on the Ring Roads, which signifies later morning rush hour periods on the weekend. In the evening, emissions in the city center are lower on the weekend, but emissions in the eastern 2nd and 3rd Ring Roads are higher because of many people shopping in the CBD on the weekend. Despite these differences, weekdays and weekend do not show any significant variability.



Figure 15. Cont.



Figure 15. Spatial comparison of carbon emissions between weekdays and weekends.

5. Conclusions

This study performed a spatiotemporal analysis of carbon emissions and taxi travel patterns in Beijing and compared weekday and weekend characteristics by processing taxi GPS data, establishing a carbon emission calculation model to calculate carbon emissions over a whole urban network, and performing their visualization based on a kernel density analysis. We fully employed the advantage of big data-mining techniques to present the dynamic spatiotemporal distribution of carbon emissions. We also converted the fuel consumption and carbon emissions to CEPK and FCPOK, respectively, all of which are global, standard, and intuitive indicators, to verify the results. The principal contributions are presented below.

- (1) The network-scale travel patterns of taxi fleets are clearly observed from taxi numbers.
- (2) The level of carbon emissions over the whole network can be evaluated via CEPK and total carbon emissions.
- (3) Although the average FCPOK we obtained from taxi GPS data is higher than expected, it can allow policy makers to issue stricter regulations on carbon emission reduction.

- (4) The average travel speed by hour can be used to monitor traffic conditions over an entire urban network. The results indicate that higher resolution travel speed data, such as the average travel speed in one minute, can be obtained to instantly monitor traffic conditions, providing that it is feasible for the hardware. The average travel speed of the entire day over the whole network is lower than the official figure, which means that the traffic situation is more serious than previously thought.
- (5) Overall, carbon emissions and travel patterns show improvements on the weekend, especially during the morning rush hour period, because most people do not commute on the weekend.
- (6) By employing the visualization method, we creatively present the spatial dynamic distribution of carbon emissions with time. Using this method, authorities can instantaneously monitor the distribution of carbon emissions.

In conclusion, these results can enable taxi companies to promote their business and management as well as supply more favorable services. These findings also allow authorities to enforce appropriate carbon emission reduction policies in order to build a more environmentally friendly society, achieve environmental protection and sustainable development, and improve living conditions, especially those related to air quality. Additionally, this study is most applicable to urban planning, infrastructure design, and the transformation of traffic modes, such as the adoption of public transport or electric vehicles to advocate low-carbon trips.

Nonetheless, there are some limitations to this research. For instance, we do not consider the speed of taxis when idling, and taxis involve relatively little carbon emissions among all travels. Furthermore, it is difficult to identify the start and end time of idling using taxi trajectory data. In addition, acceleration and deceleration are not taken into consideration because the positioning time interval of GPS data used in this study is too long to obtain more precise accelerations and decelerations. Some inevitable errors also exist in the trajectories, especially at the corner of the intersections because of positioning errors of the satellite and because the “Track intervals to line” tool in ArcGIS traces the linear distance between two points rather than the actual driving distance. Finally, the carbon emission factor exhibits a slight change with a change of speed, whereas we employ a constant number, thus leading to some errors in the calculation of carbon emissions. Further research should attempt to overcome these limitations.

Supplementary Materials: The following are available online at www.mdpi.com/1996-1073/11/3/500/s1, Video S1: Dynamic distribution of carbon emissions at different time intervals.

Acknowledgments: This work was supported by the Beijing Municipal Science and Technology Commission [grant numbers Z171100002217011]. The authors are grateful to anonymous reviewers for their valuable comments and suggestions.

Author Contributions: Jinlei Zhang and Feng Chen conceived and designed the study; Jinlei Zhang and Zijia Wang performed the research and analyzed the data; Rui Wang and Zijia Wang contributed analysis tools; Jinlei Zhang wrote the paper; Zijia Wang and Shunwei Shi revised the paper.

Conflicts of Interest: The authors declare no conflict of interest.

References

1. Yang, L.; Kwan, M.; Pan, X.; Wan, B.; Zhou, S. Scalable space-time trajectory cube for path-finding: A study using big taxi trajectory data. *Transp. Res. Part B Methodol.* **2017**, *101*, 1–27. [[CrossRef](#)]
2. Zhang, J.; Meng, W.; Liu, Q.Q.; Jiang, H.; Feng, Y.; Wang, G. Efficient vehicles path planning algorithm based on taxi GPS big data. *Opt. Int. J. Light Electron Opt.* **2016**, *127*, 2579–2585. [[CrossRef](#)]
3. Lin, N. Path Planning Method Based on Taxi Trajectory Data. *J. Inf. Comput. Sci.* **2015**, *12*, 3395–3403. [[CrossRef](#)]
4. Hu, J.; Huang, Z.; Deng, J.; Xie, H. Hierarchical Path Planning Method Based on Taxi Driver Experiences. *J. Transp. Syst. Eng. Inf. Technol.* **2013**, *13*, 185–192.

5. Li, Q.; Zeng, Z.; Zhang, T.; Li, J.; Wu, Z. Path-finding through flexible hierarchical road networks: An experiential approach using taxi trajectory data. *Int. J. Appl. Earth Obs. Geoinf.* **2011**, *13*, 110–119. [[CrossRef](#)]
6. Yuan, J.; Zheng, Y.; Zhang, C.; Xie, W.; Xie, X.; Sun, G.; Huang, Y. T-drive: Driving directions based on taxi trajectories. In Proceedings of the 18th SIGSPATIAL International Conference on Advances in Geographic Information Systems, San Jose, CA, USA, 2–5 November 2010; pp. 99–108.
7. Meng, L.; Li, R.T.; Yong, X.; Qin, Z.G. Analysis of Urban Traffic Based on Taxi GPS Data. *Lect. Notes Electr. Eng.* **2014**, *279*, 1007–1015.
8. Shan, Z.; Wang, Y.; Zhu, Q. Feasibility study of urban road traffic state estimation based on taxi GPS data. In Proceedings of the 17th IEEE International Conference on Intelligent Transportation Systems, Qingdao, China, 8–11 October 2014; pp. 2188–2193.
9. Zhang, K.; Sun, D.; Shen, S.; Zhu, Y. Analyzing spatiotemporal congestion pattern on urban roads based on taxi GPS data. *J. Transp. Land Use* **2017**, *10*, 675–694. [[CrossRef](#)]
10. Kong, X.; Yang, J.; Yang, Z. Measuring Traffic Congestion with Taxi GPS Data and Travel Time Index. In Proceedings of the 15th COTA International Conference of Transportation Professionals, Beijing, China, 24–27 July 2015.
11. Kuang, W.; An, S.; Jiang, H. Detecting Traffic Anomalies in Urban Areas Using Taxi GPS Data. *Math. Probl. Eng.* **2015**, *2015*, 809582. [[CrossRef](#)]
12. Chen, C.; Zhang, D.; Castro, P.S.; Li, N.; Sun, L.; Li, S. Real-Time Detection of Anomalous Taxi Trajectories from GPS Traces. In *Mobile and Ubiquitous Systems: Computing, Networking, and Services*; Springer: Berlin/Heidelberg, Germany, 2012.
13. Pang, L.X.; Chawla, S.; Liu, W.; Zheng, Y. On detection of emerging anomalous traffic patterns using GPS data. *Data Knowl. Eng.* **2013**, *87*, 357–373. [[CrossRef](#)]
14. Hui-Bing, L.I.; Yang, X.G.; Luo, L.H. Mining method of floating car data based on link travel time estimation. *J. Traffic Transp. Eng.* **2014**, *14*, 100–109.
15. Jiang, G.; Chang, A.; Li, Q.; Yi, F. Estimation models for average speed of traffic flow based on GPS data of taxi. *J. Southwest Jiaotong Univ.* **2011**, *46*, 638–644.
16. Zhang, H.S.; Yi, Z.; Wen, H.M.; Hu, D.C. Estimation approaches of average link travel time using GPS data. *J. Jilin Univ.* **2007**, *37*, 533–537.
17. Zhao, P.X.; Qin, K.; Zhou, Q.; Liu, C.K.; Chen, Y.X. Detecting Hotspots from Taxi Trajectory Data Using Spatial Cluster Analysis. *ISPRS Ann. Photogramm. Remote Sens. Spat. Inf. Sci.* **2015**, *II-4/W2*, 131–135. [[CrossRef](#)]
18. Chang, H.W.; Tai, Y.C.; Hsu, Y.J. Context-aware taxi demand hotspots prediction. *Int. J. Bus. Intell. Data Min.* **2010**, *5*, 3–18. [[CrossRef](#)]
19. Lee, J.; Shin, I.; Park, G.L. Analysis of the Passenger Pick-Up Pattern for Taxi Location Recommendation. In Proceedings of the International Conference on Networked Computing and Advanced Information Management, Gyeongju, Korea, 2–4 September 2008; pp. 199–204.
20. Shen, Y.; Zhao, L.; Fan, J. Analysis and Visualization for Hot Spot Based Route Recommendation Using Short-Dated Taxi GPS Traces. *Information* **2015**, *6*, 134–151. [[CrossRef](#)]
21. Xin, F.U.; Sun, M.; Sun, H. Taxi Commute Recognition and Temporal-spatial Characteristics Analysis Based on GPS Data. *China J. Highw. Transp.* **2017**, 134–143.
22. Yan-Hong, L.I.; Yuan, Z.Z.; Xie, H.H.; Cao, S.H.; Xian-Yu, W.U. Analysis on Trips Characteristics of Taxi in Suzhou Based on OD Data. *J. Transp. Syst. Eng. Inf. Technol.* **2007**, *7*, 85–89.
23. Luo, X.; Dong, L.; Dou, Y.; Zhang, N.; Ren, J.; Li, Y.; Sun, L.; Yao, S. Analysis on spatial-temporal features of taxis' emissions from big data informed travel patterns: A case of Shanghai, China. *J. Clean. Prod.* **2016**, *142*, 926–935. [[CrossRef](#)]
24. Du, Y.; Wu, J.; Yang, S.; Zhou, L. Predicting vehicle fuel consumption patterns using floating vehicle data. *J. Environ. Sci.* **2017**, *59*, 24–29. [[CrossRef](#)] [[PubMed](#)]
25. Weng, J.; Qiao, G.; Rong, J.; Chen, Z.; Liang, Q. Taxi fuel consumption and emissions estimation model based on the reconstruction of driving trajectory. *Adv. Mech. Eng.* **2017**, *9*. [[CrossRef](#)]
26. Zhao, T. On-Road Fuel Consumption Algorithm Based on Floating Car Data for Light-Duty Vehicles. Master's Thesis, Beijing Jiaotong University, Beijing, China, 2009.

27. Beijing Traffic Institute. *Report of the Fifth Beijing Urban Traffic Comprehensive Survey*; Report of Taxi Survey; Beijing Traffic Institute: Beijing, China, July 2017.
28. Jiménez-Palacios, J.L. Understanding and Quantifying Motor Vehicle Emissions with Vehicle Specific Power and TILDAS Remote Sensing. Ph.D. Thesis, Massachusetts Institute of Technology, Cambridge, MA, USA, 1999.
29. Yu, L.; Li, Z.; Qiao, F.; Li, Q. *Use Driving Simulator to Synthesize the Related Vehicle Specific Power (VSP) for Emissions and Fuel Consumption Estimations*; Journal of the Transportation Research Board: Washington, DC, USA, 31 January 2016.
30. Fukumuro, K.; Ishizaka, T.; Fukuda, A. Analysis on Relationship of Estimated VSP from Coast-down Test and Fuel Consumption. *JSTE J. Traffic Eng.* **2016**, *2*, 3235–3239.
31. Pitanuwat, S.; Sripakagorn, A. The application of VSP fuel consumption model on Hybrid and conventional vehicles in Bangkok traffic conditions. In *Proceedings of the 35th World Automotive Congress FISITA*, Maastricht, The Netherlands, 2–6 June 2014.
32. Song, G. Study on Traffic Fuel Consumptions and Emissions Model for Traffic Strategy Evaluation. Ph.D. Thesis, Beijing Jiaotong University, Beijing, China, 2008.
33. Garg, A.; Pulles, T. *2006 IPCC Guidelines for National Greenhouse Gas Inventories*; Intergovernmental Panel on Climate Change: Geneva, Switzerland, 2006; Volume 2.
34. National Bureau of Statistics of China. *China Statistical Yearbook 2016*; China Statistics Press: Beijing, China, 2016.
35. Beijing Traffic Commission. *Report of the Fifth Beijing Urban Traffic Comprehensive Survey*; General Report; Beijing Traffic Institute: Beijing, China, July 2017.



© 2018 by the authors. Licensee MDPI, Basel, Switzerland. This article is an open access article distributed under the terms and conditions of the Creative Commons Attribution (CC BY) license (<http://creativecommons.org/licenses/by/4.0/>).